Reflecting Characteristics of Anisotropic Rubber Sheets and Measurement of Complex Permittivity Tensor

OSAMU HASHIMOTO AND YASUTAKA SHIMIZU, SENIOR MEMBER, IEEE

Abstract—**Complex values of the permittivity tensor of rubber sheets which are manufactured by the rolling process were estimated by the least-squares method using the reflection coefficient measured for normal incidence. First, the frequency characteristics of the reflection coefficients of a rubber sheet backed by thin aluminum were measured from 8.5 to 10.5 GHz by changing the rolling angle relative to the incident electric field. Next, the elements of the permittivity tensor were determined by the least-squares method from many data of measured reflection coefficients of the samples.**

Five kinds of rubber sheets containing carbon particles or fibers were selected, and circular pieces 30 cm in diameter were measured by this method. The complex permittivity tensors including off-diagonal elements were thus obtained, and the principal directions of the tensor were calculated from the measured permittivity tensor. The following facts were found through this analysis: The permittivity element in the rolling direction is about five times larger and the off-diagonal elements are small compared with the diagonal elements. The principal direction of the real part is different from that of the imaginary part for a certain kind of rubber sheet mixed with carbon particles.

I. Introduction

RUBBER SHEETS mixed with carbon fibers or carbon particles can be applied to wave absorbers or shielding materials [1]. However, these materials usually have anisotropy which comes from the rolling method of manufacturing, because the carbon particles or fibers tend to be aligned along the rolling direction.

The complex permittivity tensor therefore needs to be estimated in many practical applications. In the microwave frequency range, the measurement method of tensor permeability of ferrites by means of the perturbation of cavity resonators has long been the subject of detailed investigations [2], [3]. However, these methods cannot be applied to measure the permittivity tensor of these lossy sheets because its tensor is the symmetric tensor described later.

In this paper, the complex permittivity tensor of several rubber sheets were estimated by the least-squares method using the absolute value of reflection coefficient measured for normal incidence. Five samples were selected and measured by this method. The tensor, including off-diagonal elements, was measured and the principal directions of the tensor were calculated from its measured elements.

Manuscript received January 6, 1986; revised July 11, 1986.

The authors are with Research and Development of Educational Technology, Tokyo Institute of Technology, 2-12-1 O-okayama Meguro-ku, Tokyo 152 Japan.

IEEE Log Number 86105070.

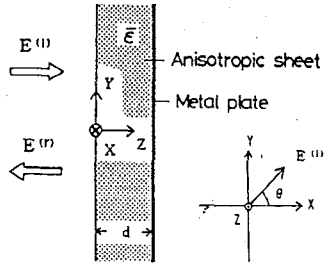

Fig. 1. (a) Lossy anisotropic sheet (b) Direction of incident electric field.

II. Method of Analysis

A. Analysis of Reflection Coefficients

In order to measure the tensor of the anisotropic sheets, the reflection coefficients from these sheets backed by a metal plate must be analyzed. The coordinate system for analysis and the direction of the direction of the incident electric field are shown in Fig. 1, where the direction of the X-axis is taken in the direction of rolling. The permittivity tensor of the sheets is assumed to take the form shown in (1), because these sheets are manufactured by the rolling method, and are therefore anisotropic only in the $X-Y$ plane

$$\tilde{\epsilon} = \begin{pmatrix} \dot{\epsilon}_{11} & \dot{\epsilon}_{12} & 0 \\ \dot{\epsilon}_{21} & \dot{\epsilon}_{22} & 0 \\ 0 & 0 & \dot{\epsilon}_{33} \end{pmatrix} \tag{1}$$

where $$\dot{\epsilon}_{12} = \dot{\epsilon}_{21}$$

where the subscripts 1, 2, and 3 denote the direction of X-, Y- and Z-axes.

First, substituting (1) into Maxwell's equations and eliminating the transverse components of the magnetic field, the following differential equation is obtained for the rubber-sheet region:

$$-\frac{\partial^2}{\partial z^2}\vec{E}_t = \omega^2 \mu_0 [\tilde{\epsilon}_t]\vec{E}_t \tag{2}$$

where $\tilde{\epsilon}_t$ is the dielectric tensor which has elements $\dot{\epsilon}_{ij}(i, j = 1, 2)$, and the subscript t denotes the transverse components.

0018-9480/86/1100-1202$01.00 ©1986 IEEE

To solve this differential equation, the transverse components of the electric field are assumed to take the following form:

$$\vec{E}_t = \begin{bmatrix} A_1 \\ A_2 \end{bmatrix} \exp(-rz)\exp(j\omega t) \tag{3}$$

where A_1 and A_2 are amplitude coefficients of E_x and E_y, and r is the propagation constant.

Next, substituting (3) into (2), an eigenvalue equation is derived and four eigenvalues $r^{(m)}$ $(m=1\cdots4)$ are obtained from four-dimensional simultaneous equations which appear in the process of solving it. Then, E_y and E_x are expressed in terms of the eigenvalue $r^{(m)}(m=1\cdots4)$

$$E_x = \sum_{m=1}^{4} B^{(m)} A_1^{(m)} \exp(-r^{(m)}z) \tag{4a}$$

$$E_y = \sum_{m=1}^{4} B^{(m)} A_2^{(m)} \exp(-r^{(m)}z) \tag{4b}$$

where $A_1^{(m)}$ and $A_2^{(m)}$ $(m=1\cdots4)$ are eigenvectors for eigenvalue $r^{(m)}$, and $B^{(m)}(m=1\cdots4)$ is the weight coefficient determined later. H_y and H_x are obtained by substituting (4a) and (4b) into Maxwell's equations

$$H_x = \frac{j}{Z_0 k_0} \sum_{m=1}^{4} B^{(m)} A_2^{(m)} r^{(m)} \exp(-r^{(m)}z) \tag{5a}$$

$$H_y = -\frac{j}{Z_0 k_0} \sum_{m=1}^{4} B^{(m)} A_1^{(m)} r^{(m)} \exp(-r^{(m)}z) \tag{5b}$$

where k_0 and Z_0 are wavenumber and characteristic impedance of free space, respectively. Using the above analysis, the electromagnetic fields in the anisotropic sheet are assumed.

Next, electromagnetic fields outside the rubber sheet $(z<0)$ are assumed to take the following equations:

$$E_{y0} = E_{\text{inc}}\left[\sin\theta\exp(-jk_0z) + \Gamma_y\exp(jk_0z)\right] \tag{6a}$$

$$E_{x0} = E_{\text{inc}}\left[\cos\theta\exp(-jk_0z) + \Gamma_x\exp(jk_0z)\right] \tag{6b}$$

$$H_{y0} = \frac{E_{\text{inc}}}{Z_0}\left[\cos\theta\exp(-jk_0z) - \Gamma_x\exp(jk_0z)\right] \tag{6c}$$

$$H_{x0} = \frac{E_{\text{inc}}}{Z_0}\left[-\sin\theta\exp(-jk_0z) + \Gamma_y\exp(jk_0z)\right] \tag{6d}$$

where E_{inc} is the amplitude coefficient of incident electric field, and Γ_x and Γ_y are the reflection coefficients of the direction of X- and Y-axes.

From the fields described above, the reflection coefficients are calculated by applying the boundary conditions that are the continuation of tangential field components. Imposing these boundary conditions on (4a)–(6d) and rearranging these equations on Γ_x, Γ_y, and $B^{(m)}$, the following simultaneous equation is obtained:

$$\begin{pmatrix} 0 & 0 & A_1^{(m)}\exp(-r^{(m)}d) \\ 0 & 0 & A_2^{(m)}\exp(-r^{(m)}d) \\ -1 & 0 & A_1^{(m)} \\ 0 & -1 & A_2^{(m)} \\ 0 & -k_0 & jA_2^{(m)}r^{(m)} \\ k_0 & 0 & -jA_1^{(m)}r^{(m)} \end{pmatrix} \begin{pmatrix} \Gamma_x \\ \Gamma_y \\ B^{(1)} \\ B^{(2)} \\ B^{(3)} \\ B^{(4)} \end{pmatrix} = \begin{pmatrix} 0 \\ 0 \\ \cos\theta \\ \sin\theta \\ -k_0\sin\theta \\ k_0\cos\theta \end{pmatrix} \tag{7}$$

where each of the third column elements is a row matrix and E_{inc} is assumed to be equal to 1. Then Γ_x and Γ_y are obtained by solving this equation. Finally, using the calculated Γ_x and Γ_y, the reflection coefficient of the direction of angle θ is calculated by the following equation:

$$\Gamma = (\Gamma_x'\cos\theta + \Gamma_y'\sin\theta) + j(\Gamma_x''\cos\theta + \Gamma_y''\sin\theta) \tag{8}$$

where

$$\Gamma_x = \Gamma_x' + j\Gamma_x''$$
$$\Gamma_y = \Gamma_y' + j\Gamma_y''.$$

B. Analysis of Tensor

Each element of the tensor is calculated by the least-squares method using reflection coefficients calculated by the method described above. First, the function F defined by the following equation is introduced:

$$F(\epsilon_1, \epsilon_2, \cdots, \epsilon_6) = \sum_{\nu=1}^{N} (\hat{X}_\nu - X_\nu)^2 \tag{9}$$

where

$$\hat{X}_\nu = 20\log|\Gamma_{\text{calc}}|_\nu, \quad X_\nu = 20\log|\Gamma_{\text{meas}}|_\nu$$

where $\epsilon_\xi(\xi=1\cdots6)$ are the real and imaginary parts of the tensor elements to be determined, and N is the number of data. $|\Gamma_{\text{calc}}|_\nu$ is calculated theoretically by the analysis described above. $|\Gamma_{\text{meas}}|_\nu$, which is the absolute value of the reflection coefficient in the same direction as the direction of incident electric field, is measured by changing the angle θ between the direction of electric field and the X-axis.

At the same time, function f_ξ is defined in order to obtain ϵ_ξ $(\xi=1\cdots6)$ by the least-squares method

$$f_\xi = \frac{\partial F}{\partial \epsilon_\xi} = 0 \qquad (\xi = 1\sim6). \tag{10}$$

The $\Delta\epsilon_\xi$ (the correction to ϵ_ξ) is obtained by solving the following simultaneous equation when the initial values ϵ_ξ' of ϵ_ξ are given:

$$[a_{\xi\eta}][\Delta\epsilon_\xi] = [b_\xi] \tag{11}$$

where

$$a_{\xi\eta} = \left(\frac{\partial f_\xi}{\partial \epsilon_\eta}\right)_{\epsilon_\xi = \epsilon_\xi'}$$

$$b_\xi = -f_\xi(\epsilon_1', \epsilon_2', \ldots, \epsilon_6') \qquad (\xi = 1\sim6,\ \eta = 1\sim6).$$

Here, the error which is contained in the most probable values $\epsilon_{0\xi}$ is calculated by the following equation because it is considered that the main error comes from the measurement of $|\Gamma_{meas}|$;

$$\sigma_\xi^2 = \sum_{\nu=1}^{N} \left(\Delta\sigma_\xi^{(\nu)}\right)^2 \tag{12}$$

where

$$\Delta\sigma_\xi^{(\nu)} = \epsilon_\xi(X_1, X_2, \cdots, X_\nu + \sigma, \cdots, X_N) - \epsilon_{0\xi}$$
$$\sigma = \sqrt{S/(N-6)}$$

and where σ is the average error which is calculated by square residual S.

III. Sample and Measurement Method

Five kinds of rubber sheets containing carbon particles or fibers were selected for the experiment. Samples $A1$, $A2$, $B1$, and $B2$ are those containing carbon particles and sample C is the sample containing carbon fibers, where the manufacturing lots of $A1$ and $A2$ are different, as are those of $B1$ and $B2$. Table I shows the thickness and content of these samples. The diameter and length of the mixed fibers are about 18 and 370 μm, respectively, and the diameter of the mixed particles is about $20 \sim 60$ μm. These samples were cut from the sheet in the form of circular pieces 30 cm in diameter and were backed by thin aluminum (Fig. 3).

The short-pulse method was used in the anechoic chamber in order to increase the accuracy of measurement for the absolute value of the reflection coefficient $|\Gamma_{meas}|_\nu$ [4], [5]. Fig. 2 and the accompanying photograph (Fig. 9) show a block diagram of the measurement of $|\Gamma_{meas}|_\nu$ and the state of measuring. In the experimental setup, in order to reduce the influence of background scattering and antenna coupling on a received signal, we use a transmitted pulse having 10-ns duration and a receiving time gate of around 10 ns, and use the separate parabolidal reflector antennas for transmitting and receiving. The reflector diameter is 60 cm and the beamwidth of the antenna is about 4° at 9.0 GHz. The distance from the antenna to the sample is about 14 m for plane wave incidence. A background noise of the measuring system is 60 dB smaller than the reflection of the metal plate which has the same size as the rubber sheet. Using this system, the absolute value of the reflection coefficient $|\Gamma_{meas}|_\nu$ was measured by changing the frequency at intervals of 0.1 GHz and the rolling angle relative to the incident electric field at intervals of 15°, as shown in Fig. 3. For sample C, the $|\Gamma_{meas}|_\nu$ was measured at angles 0, 30, 55, 60, 65, 70, 80, and 90° in order to obtain a deep minimum in it.

IV. Experimental Results

The measured values of elements $\dot{\epsilon}_{ij}$ $(= \epsilon'_{ij} - j\epsilon''_{ij}$, $i, j = 1, 2)$ and the principal directions of complex permittivity tensor are described, where each element is expressed in relative permittivity.

TABLE I
PHR: Parts Per Hundred Parts of Rubber

SAMPLE	THICKNESS (mm)	CONTENT (phr)	RANGE OF FREQUENCY (GHz)	NUMBER OF DATA
A 1	1.93	50	9.0 ~10.5	112
A 2	2.03	50	8.5 ~10.0	112
B 1	1.98	55	9.0 ~10.0	77
B 2	1.93	55	9.0 ~10.0	77
C	1.93	54	8.0 ~9.0	88

Samples for measurement.

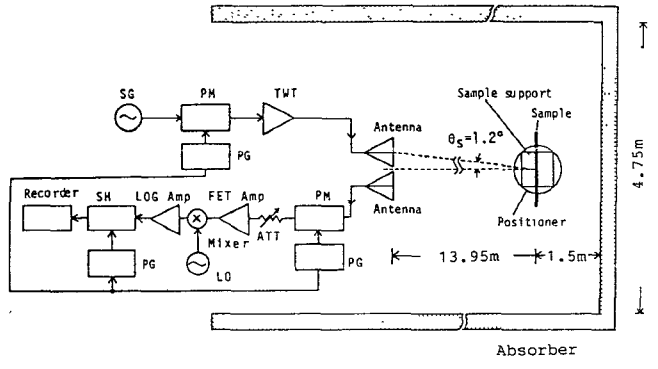

Fig. 2. Experimental setup to measure absolute value of reflection coefficient of the sample. SG, signal generator; PM, pulse modulator; TWT, traveling wave tube, PG, pulse generator; LO, local oscillator, ATT, attenuator; SH, sampling hold.

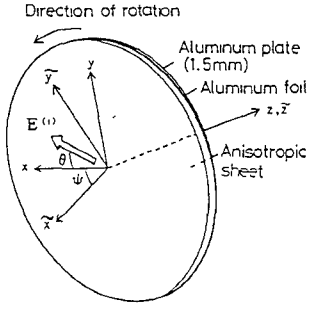

Fig. 3. Structure of the sample.

A. Permittivity Tensor

Fig. 4(a)–(d) show the measured X_ν (shown in (9)) by circles for sample $A1$, where the direction of the rolling is taken in the direction of the X-axis. Using these measured X_ν, the values of the tensors are obtained as follows:

$$\dot{\epsilon}_{11} = 17.16 - 5.88j$$
$$\dot{\epsilon}_{22} = 15.12 - 5.39j$$
$$\dot{\epsilon}_{12} = -0.089 + 0.539j \tag{13}$$

where the number of data used for measuring the tensor is 112 as shown in Table I. In these figures, the solid line shows the reflection curve calculated from the measured tensor shown in (13) and the dotted line indicates the reflection curve calculated from the tensor that is assumed to have $\dot{\epsilon}_{12} = 0$; $\dot{\epsilon}_{11}$, $\dot{\epsilon}_{22}$ are given in the right column of Table II. The diagonal elements $\dot{\epsilon}_{11}$ and $\dot{\epsilon}_{22}$ of this tensor

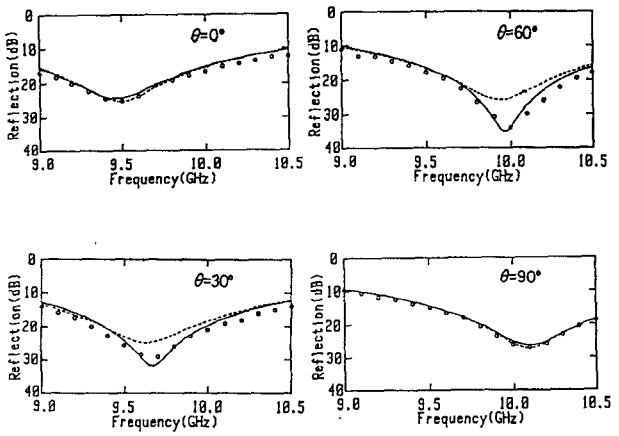

Fig. 4. Results of measured values and calculated values of absolute value of reflection coefficient in sample $A1$: o measured, — calculated ($\dot{\epsilon}_{12} \neq 0$), --- calculated ($\dot{\epsilon}_{12} = 0$).

TABLE II
THE MEASURED TENSOR ELEMENTS

SAMPLE	TENSOR ($\dot{\epsilon}_{12} \neq 0$)			TENSOR ($\dot{\epsilon}_{12} = 0$)	
	$\dot{\epsilon}_{11}$	$\dot{\epsilon}_{22}$	$\dot{\epsilon}_{12}$	$\dot{\epsilon}_{11}$	$\dot{\epsilon}_{22}$
A 1	17.16±0.05 (-5.88±0.08)j	15.12±0.05 (-5.39±0.05)j	-0.088±0.050 (+0.539±0.058)j	17.07 -5.77j	15.15 -5.31j
A 2	16.85±0.07 (-6.05±0.04)j	14.79±0.05 (-5.84±0.06)j	-0.003±0.058 (+0.805±0.051)j	16.71 -5.84j	14.81 -5.48j
B 1	17.33±0.05 (-5.73±0.03)j	16.55±0.04 (-5.51±0.03)j	+0.008±0.047 (-0.018±0.015)j	17 28 -5.75j	16.53 -5.51j
B 2	17.25±0.05 (-5.93±0.03)j	16.54±0.03 (-5.48±0.03)j	+0.015±0.051 (-0.044±0.030)j	17.28 -5.95j	16.52 -5.48j
C	118.01±7.88 (-65.68±7.18)j	22 07±0.06 (-4.33±0.04)j	-0.485±0 947 (+0.405±0 518)j	81.37 -68.44j	22.18 -4.28j

was measured at $\theta = 0$ and 90°, respectively. It is found that the solid line shows good agreement with those of the measured X_p, but the dotted line does not agree with those data because it is assumed that off-diagonal elements are equal to 0. Table II shows the tensor including off-diagonal elements calculated by this method for the other samples. It is clearly seen that $\dot{\epsilon}_{11}$ (the permittivity in the rolling direction) is about five times larger than $\dot{\epsilon}_{22}$ and off-diagonal elements are small compared with diagonal elements for sample C because the fibers are aligned along the rolling direction.

Figs. 5(a)–(c) and 6(a)–(c) show the reflection curves calculated by the measured tensor shown in Table II for sample C and $B1$, respectively. In these figures, it is found that the X_p of sample C varies significantly with the change of angle between 55–90° because the permittivity in the rolling direction is very large in it, and the dotted lines are in good agreement with the data as well as the solid line because the off-diagonal elements are small in samples C and $B1$. The errors for each tensor element, which are calculated by using (12), are evaluated to be within about ±0.5 percent for samples A and B about ±7 percent for sample C for the maximum element. Fig. 7 shows each tensor element measured and calculated in the $\tilde{X}, \tilde{Y}, \tilde{Z}$ coordinate system as shown in Fig. 3. In this figure, measured values are plotted by circles and calculated values are shown the the solid and dotted lines, where these lines were calculated by the measured tensor

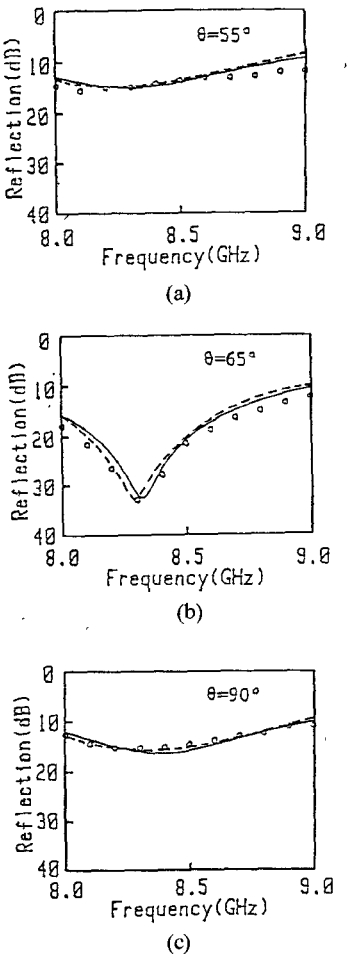

Fig. 5. Results of measured values and calculated values of absolute value of reflection coefficient in sample $C1$: o measured, — calculated ($\dot{\epsilon}_{12} \neq 0$), --- calculated ($\dot{\epsilon}_{12} = 0$).

shown in (13). The curve calculated theoretically shows agreement with measured values and each element of the tensor can be determined by this method even if off-diagonal elements are large and the direction of rolling is not known.

B. Principal Direction

Table III shows the principal directions of the tensor calculated from the measured tensor, where principal direction show the angle from the direction of rolling (X-axis). Here, the principal direction means the direction or principal axis that corresponds to a greater diagonal element and is defined for a real and an imaginary part of the tensor separately. For example, the principle direction of real part can be obtained by an angle ϕ' as follows:

$$R_{\phi'}^{-1}\begin{bmatrix}\epsilon'_{11} & \epsilon'_{12}\\ \epsilon'_{21} & \epsilon'_{22}\end{bmatrix}R_{\phi'} = \begin{bmatrix}\epsilon'_g & 0\\ 0 & \epsilon'_l\end{bmatrix} \tag{14}$$

where

$$\epsilon'_g > \epsilon'_l > 0$$

where $R_{\phi'}$ is the rotation matrix of the following form:

$$R_{\phi'} = \begin{bmatrix}\cos\phi' & -\sin\phi'\\ \sin\phi' & \cos\phi'\end{bmatrix}. \tag{15}$$

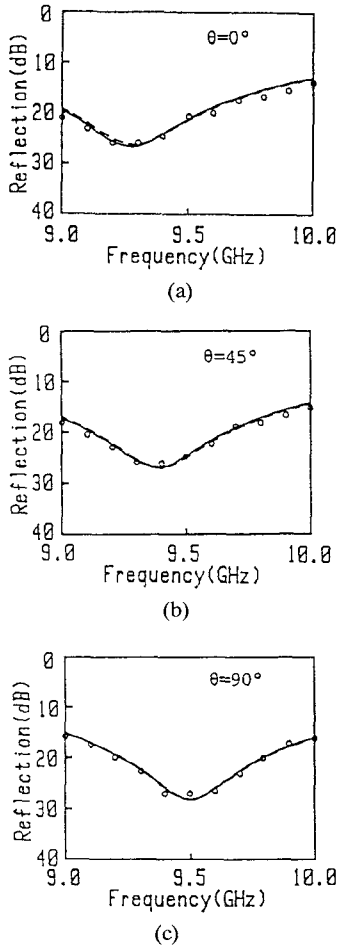

Fig. 6. Results of measured values and calculated values of absolute value of reflection coefficient in sample $B1$: o measured, — calculated ($\dot{\epsilon}_{12} \neq 0$), --- calculated ($\dot{\epsilon}_{12} = 0$).

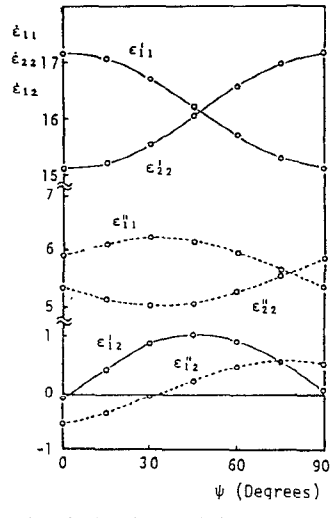

Fig. 7. Results of calculated permittivity tensor in sample $A1$: o measured, — calculated, --- calculated.

Errors in the angle are calculated from the errors in each element of the tensor as shown in Table II. The following facts are apparent from this table: The principal direction of the real part is different from that of the imaginary part for $A1$ and $A2$. The principal direction of the imaginary part is oriented at $-30 \sim -40°$ to the rolling direction. The principal directions of the real and imaginary parts almost agree with that of the rolling direction for the carbon fiber mixture. The errors in the measured principal directions for the real and imaginary parts are evaluated within about $\pm 5°$ as shown by parenthesis. Fig. 8 shows a model of the inner structure for the sheet containing carbon particles. Here, each particle is aligned almost along the direction of rolling through the rolling process, and they cling to the polymer chain that spreads like a branch. As the current flows along the branch, the principal direction for the imaginary part may be oriented to the direction of the rolling. Table IV shows the tensor and principal directions measured by changing the range of frequency. It is found that the tensor element values for the three frequency ranges agree well and the error which is caused by the frequency dispersion of the material is small for these sheets.

TABLE III
THE MEASURED PRINCIPAL DIRECTIONS

SAMPLE	PRINCIPAL DIRECTION (Deg)	
	REAL PART	IMAGINARY PART
A 1	-2.5 (-4.1~-1.1)	-32.8 (-36.1~-29.1)
A 2	-0.3 (-1.8~1.6)	-37.9 (-39.9~-35.7)
B 1	0.9 (-3.4~4.6)	4.7 (1.0~11.2)
B 2	1.2 (-3.3~5.9)	5.5 (1.6~10.4)
C	-0.3 (-0.9~0.3)	-0.4 (-1.0~0.1)

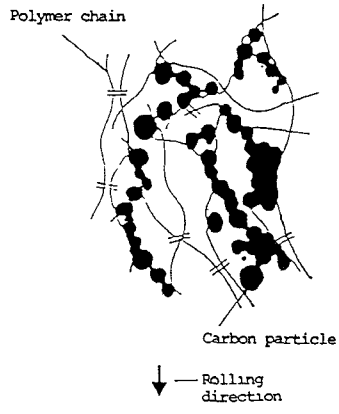

Fig. 8. Model of inner structure for sheet.

TABLE IV
TENSOR AND PRINCIPAL DIRECTIONS AS A FUNCTION OF FREQUENCY (SAMPLE: $A1$)

RANGE OF FREQUENCY (GHz)	TENSOR			PRINCIPAL DIRECTION (Deg)	
	$\dot{\epsilon}_{11}$	$\dot{\epsilon}_{22}$	$\dot{\epsilon}_{12}$	REAL PART	IMAGINARY PART
9.0 ~10.0	17.22 -5.90j	15.16 -5.42j	-0.098 +0.562j	-2.7	-33.4
9.0 ~10.5	17.16 -5.88j	15.12 -5.39j	-0.088 +0.538j	-2.5	-32.8
9.5 ~10.5	16.97 -5.94j	15.07 -5.39j	-0.088 +0.564j	-2.0	-32.0

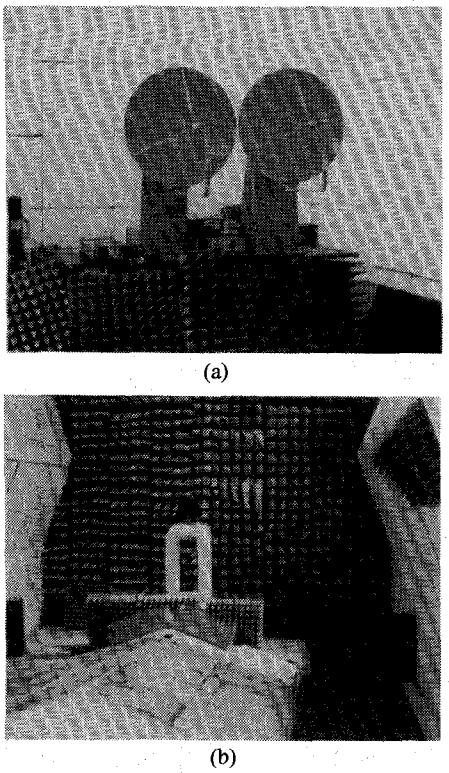

(a) (b)

Fig. 9. (a) Setup and (b) sample support for measuring the absolute value of the reflection coefficient.

V. Conclusions

The measurement of the complex permittivity tensor using the absolute value of the reflection coefficient at normal incidence was described. Five samples containing carbon particles or fibers were measured by this method. The tensor including off-diagonal elements was obtained and the principal directions were calculated from the measured tensor elements. Errors in the principal direction for the real and imaginary parts were evaluated within about $\pm 5.0°$.

The measurement method described in this paper is considered to be useful for designing a wave absorber or effective shielding.

Acknowledgment

The authors wish to thank Prof. K. Araki of Saitama University for his helpful advice and the Yokohama Rubber Co. and TDK Co. for providing the samples.

References

[1] Y. Shimizu, A. Nishikata, and S. Suzuki, "Absorbing rubber sheet mixed with carbon for *X*-band marine radar frequencies," *IECE. Japan*, vol. J68-B, pp. 928–934, 1985.

[2] W. V. Aulock and J. H. Rowen, "Measurement of dielectric and magnetic properties of ferromagnetic materials at microwave frequencies," *Bell Syst. Tech. J.*, vol. 36, no. 2, pp. 427–448, 1957.

[3] J. L. Melchor, W. P. Ayres, and H. Vartanian, "Energy concentration effects in ferrite loaded wave guides," *J. Appl. Phys.*, vol. 27, no. 1, pp. 72–77, 1956.

[4] O. Hashimoto, H. Jiromaru, Y. Watanabe, and A. Kishimoto, "A measurement method of characteristics of absorbers by short pulse," IECE. Japan, Tech. Rep. EMCJ 82-51, 1982.

[5] C. C. Tang, "Electromagnetic backscattering measurement by a time-separation method," *IRE Trans. Microwave Theory Tech.*, vol. MTT-7, pp. 209–213, Apr. 1959.

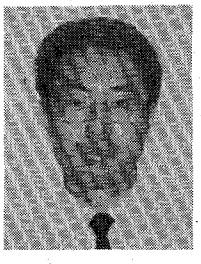

Osamu Hashimoto was born in Akita, Japan, on April 15, 1953. He received the B.E. and M.E. degrees from the University of Electro-Communications, Tokyo, Japan. He has been engaged in research on wave absorbers and shielding. Since 1983, he has been studying towards the Ph.D. degree at the Tokyo Institute of Technology, Tokyo, Japan.

Mr. Hashimoto is a member of the Institute of Electronics and Communication Engineers of Japan.

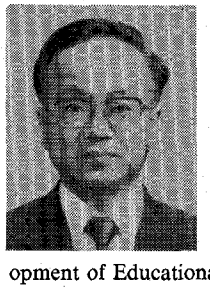

Yasutaka Shimizu (M'73–SM'82) was born in Nagano, Japan, on April 4, 1940. He received the B.E. and M.E. degrees from the Tokyo Institute of Technology, Tokyo, Japan, in 1964, and 1966, respectively, and received the Ph.D. degree in engineering through research work on microwave absorber design.

He joined the Tokyo Institute of Technology in 1970 after working at the Seiko Co., where he developed atomic frequency standards. He is also a Professor at the Center of Research and Development of Educational Technology.